Chapter 25

Deterministic diffusion

> This is a bizzare and discordant situation.
> —M.V. Berry

> (R. Artuso and P. Cvitanović)

THE ADVANCES in the theory of dynamical systems have brought a new life to Boltzmann's mechanical formulation of statistical mechanics. Sinai, Ruelle and Bowen (SRB) have generalized Boltzmann's notion of ergodicity for a constant energy surface for a Hamiltonian system in equilibrium to dissipative systems in nonequilibrium stationary states. In this more general setting the attractor plays the role of a constant energy surface, and the SRB measure of sect. 16.1 is a generalization of the Liouville measure. Such measures are purely microscopic and indifferent to whether the system is at equilibrium, close to equilibrium or far from it. "Far for equilibrium" in this context refers to systems with large deviations from Maxwell's equilibrium velocity distribution. Furthermore, the theory of dynamical systems has yielded new sets of microscopic dynamics formulas for macroscopic observables such as diffusion constants and the pressure, to which we turn now.

We shall apply cycle expansions to the analysis of *transport* properties of chaotic systems.

The resulting formulas are exact; no probabilistic assumptions are made, and the all correlations are taken into account by the inclusion of cycles of all periods. The infinite extent systems for which the periodic orbit theory yields formulas for diffusion and other transport coefficients are spatially periodic, the global state space being tiled with copies of a elementary cell. The motivation are physical problems such as beam defocusing in particle accelerators or chaotic behavior of passive tracers in $2-dimensional$ rotating flows, problems which can be described as deterministic diffusion in periodic arrays.

In sect. 25.1 we derive the formulas for diffusion coefficients in a simple physical setting, the $2-dimensional$ periodic Lorentz gas. This system, however,
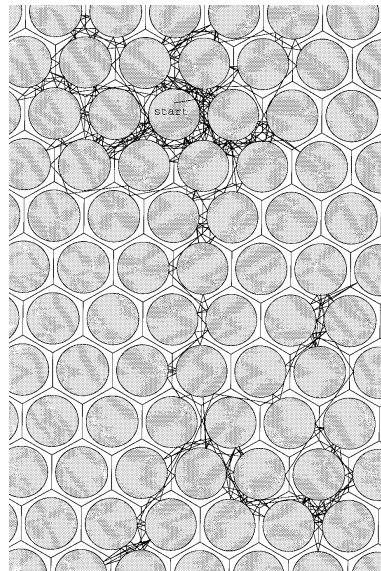
Figure 25.1: Deterministic diffusion in a finite horizon periodic Lorentz gas. (T. Schreiber)

is not the best one to illustrate the theory, due to its complicated symbolic dynamics. Therefore we apply the theory first to diffusion induced by a $1-dimensional$ maps in sect. 25.2.

25.1 Diffusion in periodic arrays

The $2-dimensional\ Lorentz\ gas$ is an infinite scatterer array in which diffusion of a light molecule in a gas of heavy scatterers is modeled by the motion of a point particle in a plane bouncing off an array of reflecting disks. The Lorentz gas is called "gas" as one can equivalently think of it as consisting of any number of pointlike fast "light molecules" interacting only with the stationary "heavy molecules" and not among themselves. As the scatterer array is built up from only defocusing concave surfaces, it is a pure hyperbolic system, and one of the simplest nontrivial dynamical systems that exhibits deterministic diffusion, figure 25.1. We shall now show that the *periodic* Lorentz gas is amenable to a purely deterministic treatment. In this class of open dynamical systems quantities characterizing global dynamics, such as the Lyapunov exponent, pressure and diffusion constant, can be computed from the dynamics restricted to the elementary cell. The method applies to any hyperbolic dynamical system that is a periodic tiling $\hat{\mathcal{M}} = \bigcup_{\hat{n} \in T} \mathcal{M}_{\hat{n}}$ of the dynamical state space $\hat{\mathcal{M}}$ by *translates* $\mathcal{M}_{\hat{n}}$ of an *elementary cell* $\mathcal{M}$, with T the abelian group of lattice translations. If the scattering array has further discrete symmetries, such as reflection symmetry, each elementary cell may be built from a *fundamental domain* $\widetilde{\mathcal{M}}$ by the action of a discrete (not necessarily abelian) group G. The symbol $\hat{\mathcal{M}}$ refers here to the full state space, i.e.,, both the spatial coordinates and the momenta. The spatial component of $\hat{\mathcal{M}}$ is the complement of the disks in the *whole* space.

We shall now relate the dynamics in $\mathcal{M}$ to diffusive properties of the Lorentz gas in $\hat{\mathcal{M}}$.
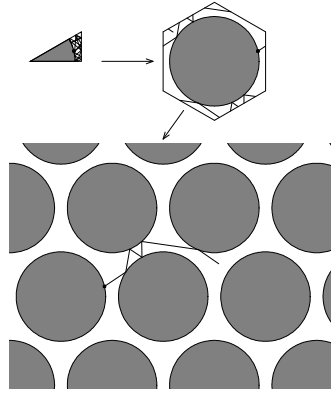
Figure 25.2: Tiling of $\hat{\mathcal{M}}$, a periodic lattice of reflecting disks, by the fundamental domain $\widetilde{\mathcal{M}}$. Indicated is an example of a global trajectory $\hat{x}(t)$ together with the corresponding elementary cell trajectory $x(t)$ and the fundamental domain trajectory $\tilde{x}(t)$. (Courtesy of J.-P. Eckmann)

These concepts are best illustrated by a specific example, a Lorentz gas based on the hexagonal lattice Sinai billiard of figure 25.2. We distinguish two types of diffusive behavior; the *infinite horizon* case, which allows for infinite length flights, and the *finite horizon* case, where any free particle trajectory must hit a disk in finite time. In this chapter we shall restrict our consideration to the finite horizon case, with disks sufficiently large so that no infinite length free flight is possible. In this case the diffusion is normal, with $\hat{x}(t)^2$ growing like t. We shall discuss the anomalous diffusion case in sect. 25.3.

As we will work with three kinds of state spaces, good manners require that we repeat what tildes, nothings and hats atop symbols signify:

> $\tilde{}$ fundamental domain, triangle in figure 25.2
>
>   elementary cell, hexagon in figure 25.2
>
> $\hat{}$ full state space, lattice in figure 25.2   (25.1)

It is convenient to define an evolution operator for each of the 3 cases of figure 25.2. $\hat{x}(t) = \hat{f}^t(\hat{x})$ denotes the point in the global space $\hat{\mathcal{M}}$ reached by the flow in time t. $x(t) = f^t(x_0)$ denotes the corresponding flow in the elementary cell; the two are related by

$$\hat{n}_t(x_0) = \hat{f}^t(x_0) - f^t(x_0) \in T \,, \tag{25.2}$$

the translation of the endpoint of the global path into the elementary cell $\mathcal{M}$. The quantity $\tilde{x}(t) = \tilde{f}^t(\tilde{x})$ denotes the flow in the fundamental domain $\widetilde{\mathcal{M}}$; $\tilde{f}^t(\tilde{x})$ is related to $f^t(\tilde{x})$ by a discrete symmetry $g \in G$ which maps $\tilde{x}(t) \in \widetilde{\mathcal{M}}$ to $x(t) \in \mathcal{M}$.   chapter 21

Fix a vector $\beta \in \mathbb{R}^d$, where d is the dimension of the state space. We will compute the diffusive properties of the Lorentz gas from the leading eigenvalue of the evolution operator (17.11)

$$s(\beta) = \lim_{t \to \infty} \frac{1}{t} \log \langle e^{\beta \cdot (\hat{x}(t) - x)} \rangle_{\mathcal{M}} \,, \tag{25.3}$$

where the average is over all initial points in the elementary cell, $x \in \mathcal{M}$.

If all odd derivatives vanish by symmetry, there is no drift and the second derivatives

$$2dD_{ij} = \left. \frac{\partial}{\partial \beta_i} \frac{\partial}{\partial \beta_j} s(\beta) \right|_{\beta=0} = \lim_{t \to \infty} \frac{1}{t} \langle (\hat{x}(t) - x)_i (\hat{x}(t) - x)_j \rangle_{\mathcal{M}} ,$$

yield a diffusion matrix. This symmetric matrix can, in general, be anisotropic (i.e., have d distinct eigenvalues and eigenvectors). The spatial diffusion constant is then given by the Einstein relation (17.13)

$$D = \frac{1}{2d} \sum_i \left. \frac{\partial^2}{\partial \beta_i^2} s(\beta) \right|_{\beta=0} = \lim_{t \to \infty} \frac{1}{2dt} \langle (\hat{q}(t) - q)^2 \rangle_{\mathcal{M}} ,$$

where the i sum is restricted to the spatial components q_i of the state space vectors $x = (q, p)$, i.e., if the dynamics is Hamiltonian, the sum is over the d the degrees of freedom.

We now turn to the connection between (25.3) and periodic orbits in the elementary cell. As the full $\hat{\mathcal{M}} \to \widetilde{\mathcal{M}}$ reduction is complicated by the non-abelian   remark 25.5
nature of G, we discuss only the abelian $\hat{\mathcal{M}} \to \mathcal{M}$ reduction.

25.1.1   Reduction from $\hat{\mathcal{M}}$ to $\mathcal{M}$

The key idea follows from inspection of the relation

$$\left\langle e^{\beta \cdot (\hat{x}(t) - x)} \right\rangle_{\mathcal{M}} = \frac{1}{|\mathcal{M}|} \int_{\substack{x \in \mathcal{M} \\ \hat{y} \in \hat{\mathcal{M}}}} dx d\hat{y} \, e^{\beta \cdot (\hat{y} - x)} \delta(\hat{y} - \hat{f}^t(x)) .$$

$|\mathcal{M}| = \int_{\mathcal{M}} dx$ is the volume of the elementary cell $\mathcal{M}$. Due to translational symmetry, it suffices to start with a density of trajectories defined over a single elementary cell $\mathcal{M}$. As in sect. 17.2, we have used the identity $1 = \int_{\mathcal{M}} dy \, \delta(y - \hat{x}(t))$ to motivate the introduction of the evolution operator $\mathcal{L}^t(\hat{y}, x)$. There is a unique lattice translation $\hat{n}$ such that $\hat{y} = y - \hat{n}$, with the endpoint $y \in \mathcal{M}$ translated back to the elementary cell, and $f^t(x)$ given by (25.2). The difference is a translation by a constant lattice vector $\hat{n}$, and the Jacobian for changing integration from $d\hat{y}$ to dy equals unity. Therefore, and this is the main point, translation invariance can be used to reduce this average to the elementary cell:

$$\langle e^{\beta \cdot (\hat{x}(t) - x)} \rangle_{\mathcal{M}} = \frac{1}{|\mathcal{M}|} \int_{x,y \in \mathcal{M}} dx dy \, e^{\beta \cdot (\hat{f}^t(x) - x)} \delta(y - f^t(x)) . \tag{25.4}$$

As this is a translation, the Jacobian is $|\partial \hat{y} / \partial y| = 1$. In this way the global $\hat{f}^t(x)$ flow, infinite volume state space averages can be computed by following the flow

$f^t(x_0)$ restricted to the compact, finite volume elementary cell $\mathcal{M}$. The equation (25.4) suggests that we study the evolution operator

$$\mathcal{L}^t(y, x) = e^{\beta \cdot (\hat{x}(t) - x)} \delta(y - f^t(x)), \tag{25.5}$$

where $\hat{x}(t) = \hat{f}^t(x) \in \hat{\mathcal{M}}$ is the displacement in the full space, but x, $f^t(x)$, $y \in \mathcal{M}$. It is straightforward to check that this operator satisfies the semigroup property (17.25),

$$\int_{\mathcal{M}} dz\, \mathcal{L}^{t_2}(y, z) \mathcal{L}^{t_1}(z, x) = \mathcal{L}^{t_2 + t_1}(y, x) .$$

For $\beta = 0$, the operator (25.5) is the Perron-Frobenius operator (16.10), with the leading eigenvalue $e^{s_0} = 1$ because there is no escape from this system (see the flow conservation sum rule (22.11)).

The rest is old hat. The spectrum of $\mathcal{L}$ is evaluated by taking the trace section 18.2

$$\operatorname{tr} \mathcal{L}^t = \int_{\mathcal{M}} dx\, e^{\beta \cdot \hat{n}_t(x)} \delta(x - x(t)) .$$

Here $\hat{n}_t(x)$ is the discrete lattice translation defined in (25.2). Two kinds of orbits periodic in the elementary cell contribute. A periodic orbit is called *standing* if it is also periodic orbit of the infinite state space dynamics, $\hat{f}^{T_P}(x) = x$, and it is called *running* if it corresponds to a lattice translation in the dynamics on the infinite state space, $\hat{f}^{T_P}(x) = x + \hat{n}_p$. We recognize the shortest repeating segment of a running orbit as our old 'relative periodic orbit' friend from chapter 9. In the theory of area–preserving maps such as the standard map of example 7.6 these orbits are called *accelerator modes*, as the diffusion takes place along the momentum rather than the position coordinate. The traveled distance $\hat{n}_p = \hat{n}_{T_p}(x_0)$ is independent of the starting point x_0, as can be easily seen by continuing the path periodically in $\hat{\mathcal{M}}$.

The final result is the spectral determinant (19.6)

$$\det(s(\beta) - \mathcal{A}) = \prod_p \exp\left(-\sum_{r=1}^{\infty} \frac{1}{r} \frac{e^{(\beta \cdot \hat{n}_p - sT_p)r}}{\left|\det\left(\mathbf{1} - M_p^r\right)\right|}\right), \tag{25.6}$$

or the corresponding dynamical zeta function (19.15)

$$1/\zeta(\beta, s) = \prod_p \left(1 - \frac{e^{(\beta \cdot \hat{n}_p - sT_p)}}{|\Lambda_p|}\right) . \tag{25.7}$$

The dynamical zeta function cycle averaging formula (20.21) for the diffusion constant (17.13), zero mean drift $\langle \hat{x}_i \rangle = 0$, is given by

$$D = \frac{1}{2d} \frac{\langle \hat{x}^2 \rangle_\zeta}{\langle T \rangle_\zeta} = \frac{1}{2d} \frac{1}{\langle T \rangle_\zeta} \sum' \frac{(-1)^{k+1}(\hat{n}_{p_1} + \cdots + \hat{n}_{p_k})^2}{|\Lambda_{p_1} \cdots \Lambda_{p_k}|} . \qquad (25.8)$$

where the sum is over all distinct non-repeating combination of prime cycles. The derivation is standard, still the formula is strange. Diffusion is unbounded motion across an infinite lattice; nevertheless, the reduction to the elementary cell enables us to compute relevant quantities in the usual way, in terms of periodic orbits.

A sleepy reader might protest that $x(T_p) - x(0)$ is manifestly equal to zero for a periodic orbit. That is correct; $\hat{n}_p$ in the above formula refers to a displacement $\hat{x}(T_p)$ on the *infinite* periodic lattice, while p refers to closed orbit of the dynamics $f^t(x)$ reduced to the elementary cell, with x_p a periodic point in the closed prime cycle p.

Even so, this is not an obvious formula. Globally periodic orbits have $\hat{x}_p^2 = 0$, and contribute only to the time normalization $\langle T \rangle_\zeta$. The mean square displacement $\langle \hat{x}^2 \rangle_\zeta$ gets contributions only from the periodic runaway trajectories; they are closed in the elementary cell, but on the periodic lattice each one grows like $\hat{x}(t)^2 = (\hat{n}_p/T_p)^2 t^2 = v_p^2 t^2$. So the orbits that contribute to the trace formulas and spectral determinants exhibit either ballistic transport or no transport at all: diffusion arises as a balance between the two kinds of motion, weighted by the $1/|\Lambda_p|$ measure. If the system is not hyperbolic such weights may be abnormally large, with $1/|\Lambda_p| \approx 1/T_p^\alpha$ rather than $1/|\Lambda_p| \approx e^{-T_p \lambda}$, where λ is the Lyapunov exponent, and they may lead to anomalous diffusion - accelerated or slowed down depending on whether the probabilities of the running or the standing orbits are enhanced.

section 25.3

We illustrate the main idea, tracking of a globally diffusing orbit by the associated confined orbit restricted to the elementary cell, with a class of simple $1-dimensional$ dynamical systems where all transport coefficients can be evaluated analytically.

25.2 Diffusion induced by chains of $1 - dimensional$ maps

In a typical deterministic diffusive process, trajectories originating from a given scatterer reach a finite set of neighboring scatterers in one bounce, and then the process is repeated. As was shown in chapter 11, the essential part of this process is the stretching along the unstable directions of the flow, and in the crudest approximation the dynamics can be modeled by $1-dimensional$ expanding maps. This observation motivates introduction of a class of particularly simple $1-dimensional$ systems.
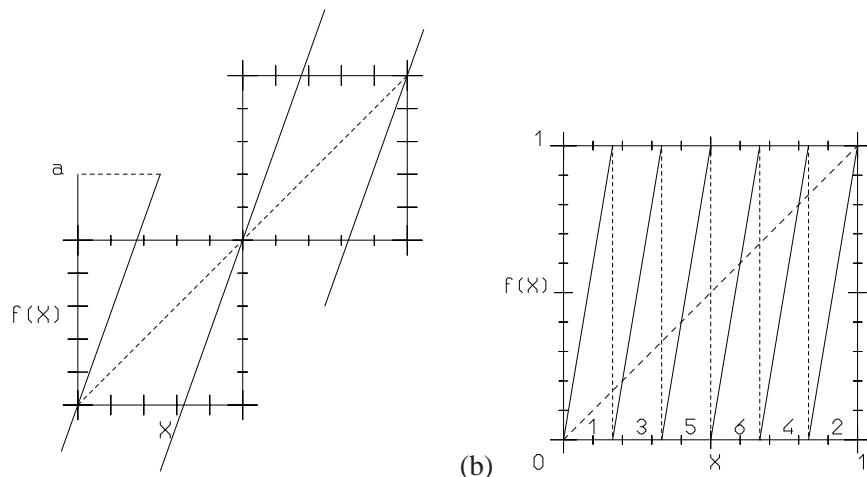
Figure 25.3: (a) $\hat{f}(\hat{x})$, the full space sawtooth map (25.9), $\Lambda > 2$. (b) $f(x)$, the sawtooth map restricted to the unit circle (25.12), $\Lambda = 6$.

(a)

(b)

Example 25.1 *Chains of piecewise linear maps.* *We start by defining the map $\hat{f}$ on the unit interval as*

$$\hat{f}(\hat{x}) = \begin{cases} \Lambda\hat{x} & \hat{x} \in [0, 1/2) \\ \Lambda\hat{x} + 1 - \Lambda & \hat{x} \in (1/2, 1] \end{cases} , \qquad \Lambda > 2, \tag{25.9}$$

and then extending the dynamics to the entire real line, by imposing the translation property

$$\hat{f}(\hat{x} + \hat{n}) = \hat{f}(\hat{x}) + \hat{n} \qquad \hat{n} \in \mathbb{Z}. \tag{25.10}$$

As the map is discontinuous at $\hat{x} = 1/2$, $\hat{f}(1/2)$ is undefined, and the $x = 1/2$ point has to be excluded from the Markov partition. The map is antisymmetric under the $\hat{x}$-coordinate flip

$$\hat{f}(\hat{x}) = -\hat{f}(-\hat{x}), \tag{25.11}$$

so the dynamics will exhibit no mean drift; all odd derivatives of the generating function (17.11) with respect to β, evaluated at $\beta = 0$, will vanish.

  The map (25.9) is sketched in figure 25.3 (a). Initial points sufficiently close to either of the fixed points in the initial unit interval remain in the elementary cell for one iteration; depending on the slope Λ, other points jump $\hat{n}$ cells, either to the right or to the left. Repetition of this process generates a random walk for almost every initial condition.

  The translational symmetry (25.10) relates the unbounded dynamics on the real line to dynamics restricted to the elementary cell - in the example at hand, the unit interval curled up into a circle. Associated to $\hat{f}(\hat{x})$ we thus also consider the circle map

$$f(x) = \hat{f}(\hat{x}) - \left[\hat{f}(\hat{x})\right], \qquad x = \hat{x} - [\hat{x}] \in [0, 1] \tag{25.12}$$

figure 25.3 (b), where $[\cdots]$ stands for the integer part (25.2). For the piecewise linear map of figure 25.3 we can evaluate the dynamical zeta function in closed form. Each branch has the same value of the slope, and the map can be parameterized by a single parameter, for example its critical value $a = \hat{f}(1/2)$, the absolute maximum on the interval $[0, 1]$ related to the slope of the map by $a = \Lambda/2$. The larger Λ is, the stronger is the stretching action of the map.

As noted in sect. 25.1.1, the elementary cell cycles correspond to either standing or running orbits for the map on the full line: we shall refer to $\hat{n}_p \in \mathbb{Z}$ as the *jumping number* of the p cycle, and take as the cycle weight

$$t_p = z^{n_p} e^{\beta \hat{n}_p}/|\Lambda_p|. \tag{25.13}$$

The diffusion constant formula (25.8) for $1-dimensional$ maps is

$$D = \frac{1}{2} \frac{\left\langle \hat{n}^2 \right\rangle_\zeta}{\langle n \rangle_\zeta}, \tag{25.14}$$

where the "mean cycle time" is given by (20.22)

$$\langle n \rangle_\zeta = z \frac{\partial}{\partial z} \frac{1}{\zeta(0, z)} \bigg|_{z=1} = -\sum' (-1)^k \frac{n_{p_1} + \cdots + n_{p_k}}{|\Lambda_{p_1} \cdots \Lambda_{p_k}|}, \tag{25.15}$$

and the "mean cycle displacement squared" by (20.25)

$$\left\langle \hat{n}^2 \right\rangle_\zeta = \frac{\partial^2}{\partial \beta^2} \frac{1}{\zeta(\beta, 1)} \bigg|_{\beta=0} = -\sum' (-1)^k \frac{(\hat{n}_{p_1} + \cdots + \hat{n}_{p_k})^2}{|\Lambda_{p_1} \cdots \Lambda_{p_k}|}, \tag{25.16}$$

the primed sum indicating all distinct non-repeating combinations of prime cycles. The evaluation of these formulas for the simple system of example 25.1 will require nothing more than pencil and paper.

Example 25.2 *Unrestricted symbolic dynamics.* *Whenever Λ is an integer number, the symbolic dynamics is exceedingly simple. For example, for the case $\Lambda = 6$ illustrated in figure 25.3 (b), the elementary cell map consists of 6 full branches, with uniform stretching factor $\Lambda = 6$. The branches have different jumping numbers: for branches 1 and 2 we have $\hat{n} = 0$, for branch 3 we have $\hat{n} = +1$, for branch 4 $\hat{n} = -1$, and finally for branches 5 and 6 we have respectively $\hat{n} = +2$ and $\hat{n} = -2$. The same structure reappears whenever Λ is an even integer $\Lambda = 2a$: all branches are mapped onto the whole unit interval and we have two $\hat{n} = 0$ branches, one branch for which $\hat{n} = +1$ and one for which $\hat{n} = -1$, and so on, up to the maximal jump $|\hat{n}| = a - 1$. The symbolic dynamics is thus full, unrestricted shift in $2a$ symbols $\{0_+, 1_+, \ldots, (a-1)_+, (a-1)_-, \ldots, 1_-, 0_-\}$, where the symbol indicates both the length and the direction of the corresponding jump.*

For the piecewise linear maps with uniform stretching the weight associated with a given symbol sequence is a product of weights for individual steps, $t_{sq} = t_s t_q$. For the map of figure 25.3 there are 6 distinct weights (25.13):

$$
\begin{aligned}
t_1 &= t_2 = z/\Lambda \\
t_3 &= e^\beta z/\Lambda, \quad t_4 = e^{-\beta} z/\Lambda, \quad t_5 = e^{2\beta} z/\Lambda, \quad t_6 = e^{-2\beta} z/\Lambda.
\end{aligned}
$$

The piecewise linearity and the simple symbolic dynamics lead to the full cancelation of all curvature corrections in (20.7). The exact *dynamical zeta function (15.15) is given by the fixed point contributions:*

$$
\begin{aligned}
1/\zeta(\beta, z) &= 1 - t_{0_+} - t_{0_-} - \cdots - t_{(a-1)_+} - t_{(a-1)_-} \\
&= 1 - \frac{z}{a}\left(1 + \sum_{j=1}^{a-1} \cosh(\beta j)\right).
\end{aligned}
\tag{25.17}
$$

The leading (and only) eigenvalue of the evolution operator (25.5) is

$$
s(\beta) = \log\left\{\frac{1}{a}\left(1 + \sum_{j=1}^{a-1} \cosh(\beta j)\right)\right\}, \qquad \Lambda = 2a, \ a \text{ integer}.
\tag{25.18}
$$

The flow conservation (22.11) sum rule is manifestly satisfied, so $s(0) = 0$. The first derivative $s(0)'$ vanishes as well by the left/right symmetry of the dynamics, implying vanishing mean drift $\langle \hat{x} \rangle = 0$. The second derivative $s(\beta)''$ yields the diffusion constant (25.14):

$$
\langle n \rangle_\zeta = 2a\frac{1}{\Lambda} = 1, \qquad \left\langle \hat{x}^2 \right\rangle_\zeta = 2\frac{0^2}{\Lambda} + 2\frac{1^2}{\Lambda} + 2\frac{2^2}{\Lambda} + \cdots + 2\frac{(a-1)^2}{\Lambda}
\tag{25.19}
$$

Using the identity $\sum_{k=1}^{n} k^2 = n(n+1)(2n+1)/6$ we obtain

$$
D = \frac{1}{24}(\Lambda - 1)(\Lambda - 2), \qquad \Lambda \text{ even integer}.
\tag{25.20}
$$

Similar calculation for odd integer $\Lambda = 2k - 1$ yields

exercise 25.1

$$
D = \frac{1}{24}(\Lambda^2 - 1), \qquad \Lambda \text{ odd integer}.
\tag{25.21}
$$

25.2.1 Higher order transport coefficients

The same approach yields higher order transport coefficients

$$
\mathcal{B}_k = \frac{1}{k!}\frac{d^k}{d\beta^k}s(\beta)\bigg|_{\beta=0}, \qquad \mathcal{B}_2 = D,
\tag{25.22}
$$

known for $k > 2$ as the Burnett coefficients. The behavior of the higher order coefficients yields information on the relaxation to the asymptotic distribution function generated by the diffusive process. Here $\hat{x}_t$ is the relevant dynamical variable and $\mathcal{B}_k$'s are related to moments $\left\langle \hat{x}_t^k \right\rangle$ of arbitrary order.

Were the diffusive process purely Gaussian

$$
e^{ts(\beta)} = \frac{1}{\sqrt{4\pi Dt}} \int_{-\infty}^{+\infty} d\hat{x}\, e^{\beta\hat{x}} e^{-\hat{x}^2/(4Dt)} = e^{\beta^2 Dt}
\tag{25.23}
$$

the only $\mathcal{B}_k$ coefficient different from zero would be $\mathcal{B}_2 = D$. Hence, nonvanishing higher order coefficients signal deviations of deterministic diffusion from a Gaussian stochastic process.

diffusion - 12jan2009   ChaosBook.org version13.3, Sep 23 2010

Figure 25.4: (a) A partition of the unit interval into six intervals, labeled by the jumping number $\hat{n}(x)$ $I = \{0_+, 1_+, 2_+, 2_-, 1_-, 0_-\}$. The partition is Markov, as the critical point is mapped onto the right border of $\mathcal{M}_{1_+}$. (b) The transition graph for this partition. (c) The transition graph in the compact notation of (25.26) (introduced by Vadim Moroz).
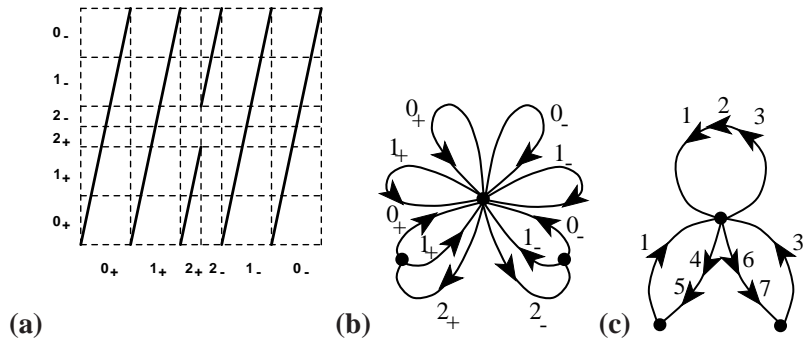
Example 25.3 $\mathcal{B}_4$ **Burnett coefficient.** *For the map under consideration the first Burnett coefficient coefficient $\mathcal{B}_4$ is easily evaluated. For example, using (25.18) in the case of even integer slope $\Lambda = 2a$ we obtain*

$$\mathcal{B}_4 = -\frac{1}{4! \cdot 60}(a-1)(2a-1)(4a^2 - 9a + 7). \tag{25.24}$$

We see that deterministic diffusion is <u>not</u> a Gaussian stochastic process. Higher order even coefficients may be calculated along the same lines.

25.2.2 Finite Markov partitions

For piecewise-linear maps exact results may be obtained whenever the critical points are mapped in finite numbers of iterations onto partition boundary points, or onto unstable periodic orbits. We will work out here an example for which this occurs in two iterations, leaving other cases as exercises. The key idea is to construct a *Markov partition* (11.2), with intervals mapped *onto* unions of intervals.

Example 25.4 *A finite Markov partition.* *As an example we determine a value of the parameter $4 \leq \Lambda \leq 6$ for which $f(f(1/2)) = 0$. As in the integer Λ case, we partition the unit interval into six intervals, labeled by the jumping number $\hat{n}(x) \in \{\mathcal{M}_{0_+}, \mathcal{M}_{1_+}, \mathcal{M}_{2_+}, \mathcal{M}_{2_-}, \mathcal{M}_{1_-}, \mathcal{M}_{0_-}\}$, ordered by their placement along the unit interval, figure 25.4 (a).*

In general the critical value $a = \hat{f}(1/2)$ will not correspond to an interval border, but now we choose a such that the critical point is mapped onto the right border of $\mathcal{M}_{1_+}$. Equating $f(1/2)$ with the right border of $\mathcal{M}_{1_+}$, $x = 1/\Lambda$, we obtain a quadratic equation with the expanding solution $\Lambda = 2(\sqrt{2}+1)$. For this parameter value $f(\mathcal{M}_{1_+}) = \mathcal{M}_{0_+} \bigcup \mathcal{M}_{1_+}$, $f(\mathcal{M}_{2_-}) = \mathcal{M}_{0_-} \bigcup \mathcal{M}_{1_-}$, while the remaining intervals map onto the whole unit interval $\mathcal{M}$. The transition matrix (14.1) is given by

$$\phi' = T\phi = \begin{pmatrix} 1 & 1 & 1 & 0 & 1 & 1 \\ 1 & 1 & 1 & 0 & 1 & 1 \\ 1 & 1 & 0 & 0 & 1 & 1 \\ 1 & 1 & 0 & 0 & 1 & 1 \\ 1 & 1 & 0 & 1 & 1 & 1 \\ 1 & 1 & 0 & 1 & 1 & 1 \end{pmatrix} \begin{pmatrix} \phi_{0_+} \\ \phi_{1_+} \\ \phi_{2_+} \\ \phi_{2_-} \\ \phi_{1_-} \\ \phi_{0_-} \end{pmatrix}. \tag{25.25}$$

One could diagonalize (25.25) on a computer, but, as we saw in chapter 14, the transition graph of figure 25.4 (b) corresponding to map figure 25.4 (a) offers more insight into the dynamics. Figure 25.4 (b) can be redrawn more compactly as transition graph figure 25.4 (c) by replacing parallel lines in a graph by their sum

$$= t_1 + t_2 + t_3 . \qquad (25.26)$$

The dynamics is unrestricted in the alphabet

$$\mathcal{A} = \{0_+, \ 1_+, \ 2_+0_+, \ 2_+1_+, \ 2_-1_-, \ 2_-0_-, \ 1_-, \ 0_-\} .$$

Applying the loop expansion (15.15) of sect. 15.3, we are led to the dynamical zeta function

$$
\begin{aligned}
1/\zeta(\beta, z) \ &= \ 1 - t_{0_+} - t_{1_+} - t_{2_+0_+} - t_{2_+1_+} - t_{2_-1_-} - t_{2_-0_-} - t_{1_-} - t_{0_-} \\
&= \ 1 - \frac{2z}{\Lambda} \left(1 + \cosh(\beta)\right) - \frac{2z^2}{\Lambda^2} \left(\cosh(2\beta) + \cosh(3\beta)\right) . \qquad (25.27)
\end{aligned}
$$

For grammar as simple as this one, the dynamical zeta function is the sum over fixed points of the unrestricted alphabet. As the first check of this expression for the dynamical zeta function we verify that

$$1/\zeta(0, 1) = 1 - \frac{4}{\Lambda} - \frac{4}{\Lambda^2} = 0 ,$$

as required by the flow conservation (22.11). Conversely, we could have started by picking the desired Markov partition, writing down the corresponding dynamical zeta function, and then fixing Λ by the $1/\zeta(0, 1) = 0$ condition. For more complicated transition graphs this approach, together with the factorization (25.35), is helpful in reducing the order of the polynomial condition that fixes Λ.

The diffusion constant follows from (25.14)   exercise 25.3

$$
\langle n \rangle_\zeta \ = \ 4\frac{1}{\Lambda} + 4\frac{2}{\Lambda^2} , \quad \left\langle \hat{n}^2 \right\rangle_\zeta \ = \ 2\frac{1^2}{\Lambda} + 2\frac{2^2}{\Lambda^2} + 2\frac{3^2}{\Lambda^2}
$$

$$
D \ = \ \frac{15 + 2\sqrt{2}}{16 + 8\sqrt{2}} . \qquad (25.28)
$$

It is by now clear how to build an infinite hierarchy of finite Markov partitions: tune the slope in such a way that the critical value $f(1/2)$ is mapped into the fixed point at the origin in a finite number of iterations $p \ f^P(1/2) = 0$. By taking higher and higher values of p one constructs a dense set of Markov parameter values, organized into a hierarchy that resembles the way in which rationals are densely embedded in the unit interval. For example, each of the 6 primary intervals can be subdivided into 6 intervals obtained by the 2-nd iterate of the map, and for the critical point mapping into any of those in 2 steps the grammar (and the corresponding cycle expansion) is finite. So, if we can prove continuity of $D = D(\Lambda)$, we can apply the periodic orbit theory to the sawtooth map (25.9) for a random "generic" value of the parameter Λ, for example $\Lambda = 4.5$. The idea is to bracket this value of Λ by a sequence of nearby Markov values, compute the exact diffusion constant for each such Markov partition, and study their convergence
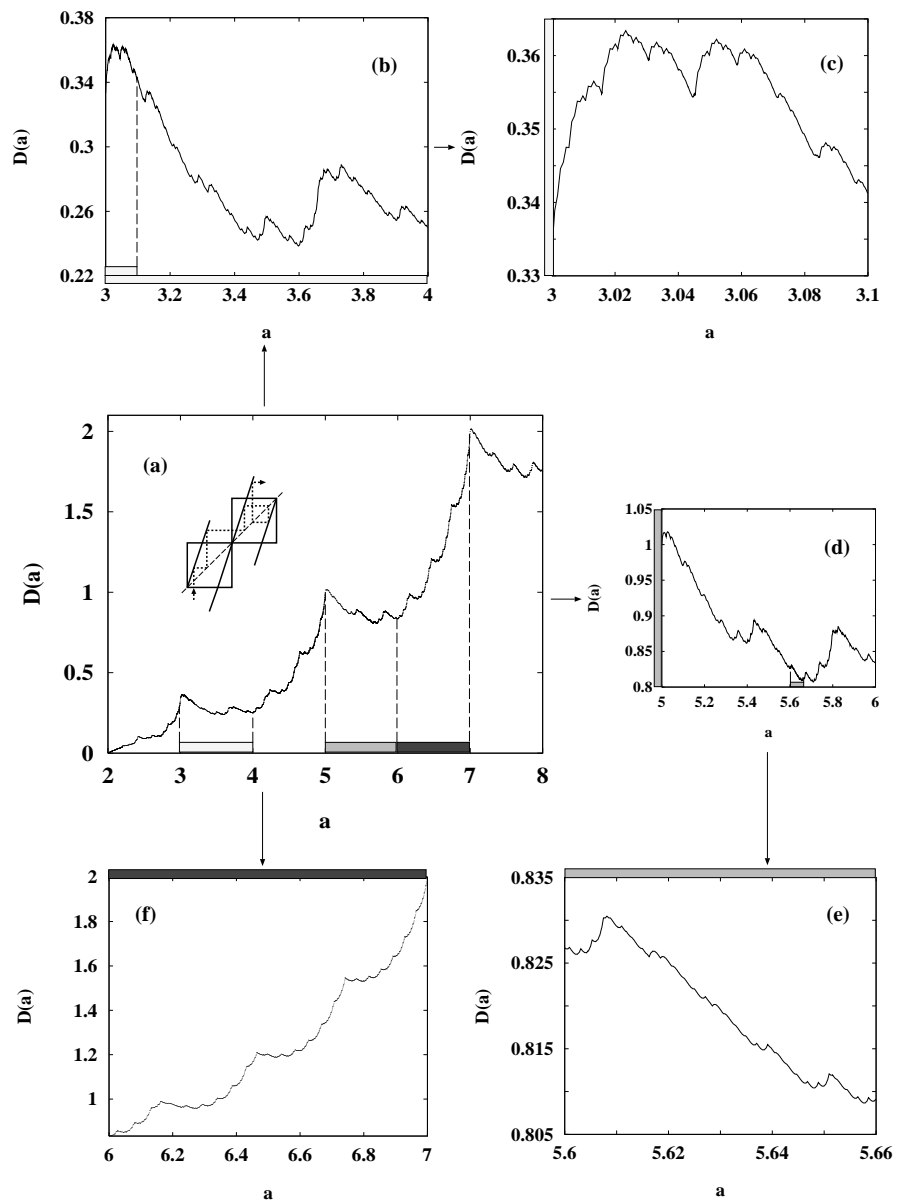
Figure 25.5: The dependence of D on the map parameter a is continuous, but not monotone. Here a stands for the slope Λ in (25.9). (From ref. [25.9].)

toward the value of D for $\Lambda = 4.5$. Judging how difficult such problem is already for a tent map (see sect. 15.5), this is not likely to take only a week of work.

Expressions like (25.20) may lead to an expectation that the diffusion coefficient (and thus transport properties) are smooth functions of parameters controlling the chaoticity of the system. For example, one might expect that the diffusion coefficient increases smoothly and monotonically as the slope Λ of the map (25.9) is increased, or, perhaps more physically, that the diffusion coefficient is a smooth function of the Lyapunov exponent λ. This turns out not to be true: D as a function of Λ is a fractal, nowhere differentiable curve illustrated in figure 25.5. The dependence of D on the map parameter Λ is rather unexpected - even though for larger Λ more points are mapped outside the unit cell in one iteration, the diffusion constant does not necessarily grow.
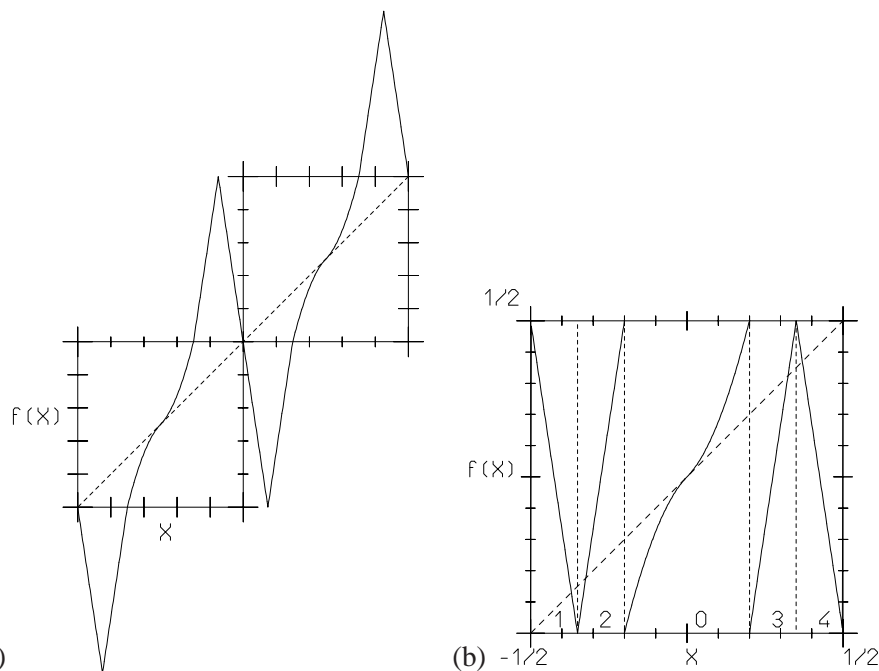
Figure 25.6: (a) A map with marginal fixed point. (b) The map restricted to the unit circle.   (a)   (b)

This is a consequence of the lack of structural stability, even of purely hyperbolic systems such as the Lozi map and the $1 - dimensional$ diffusion map (25.9). The trouble arises due to non-smooth dependence of the topological entropy on system parameters - any parameter change, no mater how small, leads to creation and destruction of infinitely many periodic orbits. As far as diffusion is concerned this means that even though local expansion rate is a smooth function of Λ, the number of ways in which the trajectory can re-enter the initial cell is an irregular function of Λ.

The lesson is that lack of structural stability implies lack of spectral stability, and no global observable is expected to depend smoothly on the system parameters. If you want to master the material, working through one of the deterministic diffusion projects on ChaosBook.org/pages is strongly recommended.

25.3 Marginal stability and anomalous diffusion

What effect does the intermittency of chapter 24 have on transport properties? A marginal fixed point affects the balance between the running and standing orbits, thus generating a mechanism that may result in anomalous diffusion.

Example 25.5 Anomalous diffusion. *Consider a* $1-dimensional$ *map of the real line on itself shown in figure 25.6 (a), with the same properties as in sect. 25.2, except for a marginal fixed point at* $x = 0$. *The corresponding circle map is given in figure 25.6 (b). As in sect. 24.2.1, a branch with support in* $\mathcal{M}_i$, $i = 1, 2, 3, 4$ *has constant slope* Λ_i, *while* $f|_{\mathcal{M}_0}$ *is of intermittent form. To keep you nimble, this time we take a slightly different choice of slopes. The toy example of sect. 24.2.1 was cooked up so that the*

$1/s$ branch cut in dynamical zeta function was the whole answer. Here we shall take a slightly different route, and pick piecewise constant slopes such that the dynamical zeta function for intermittent system can be expressed in terms of the Jonquière function remark 25.7

$$J(z, s) = \sum_{k=1}^{\infty} z^k/k^s. \tag{25.29}$$

Once the $\overline{0}$ fixed point is pruned away, the symbolic dynamics is given by the infinite alphabet $\{1, 2, 3, 4, 0^i1, 0^j2, 0^k3, 0^l4\}$, $i, j, k, l = 1, 2, \ldots$ (compare with table 24.1). The partitioning of the subinterval $\mathcal{M}_0$ is induced by $\mathcal{M}_{0^k(right)} = \hat{f}^{-k}_{(right)}(\mathcal{M}_3 \bigcup \mathcal{M}_4)$ (where $\hat{f}^{-1}_{(right)}$ denotes the inverse of the right branch of $\hat{f}|_{\mathcal{M}_0}$) and the same reasoning applies to the leftmost branch. These are regions over which the slope of $\hat{f}|_{\mathcal{M}_0}$ is constant. Thus we have the following stabilities and jumping numbers associated to letters:

$$
\begin{array}{lll}
0^k3, 0^k4 & \Lambda_p = \frac{k^{1+\alpha}}{q/2} & \hat{n}_p = 1 \\[2mm]
0^l1, 0^l2 & \Lambda_p = \frac{l^{1+\alpha}}{q/2} & \hat{n}_p = -1 \\[2mm]
3, 4 & \Lambda_p = \pm\Lambda & \hat{n}_p = 1 \\[2mm]
2, 1 & \Lambda_p = \pm\Lambda & \hat{n}_p = -1 \, ,
\end{array}
\tag{25.30}
$$

where $\alpha = 1/s$ is determined by the intermittency exponent (24.1), while q is to be determined by the flow conservation (22.11) for $\hat{f}$:

$$\frac{4}{\Lambda} + 2q\zeta(\alpha + 1) = 1$$

(where ζ is the Riemann zeta function), so that $q = (\Lambda - 4)/(2\Lambda\zeta(\alpha + 1))$. The dynamical zeta function picks up contributions just by the alphabet's letters, as we have imposed piecewise linearity, and can be expressed in terms of a Jonquière function (25.29):

$$1/\zeta_0(z, \beta) = 1 - \frac{4}{\Lambda}z\cosh\beta - \frac{\Lambda - 4}{\Lambda\zeta(1 + \alpha)}z\cosh\beta \cdot J(z, \alpha + 1). \tag{25.31}$$

Its first zero $z(\beta)$ is determined by

$$\frac{4}{\Lambda}z + \frac{\Lambda - 4}{\Lambda\zeta(1 + \alpha)}z \cdot J(z, \alpha + 1) = \frac{1}{\cosh\beta}.$$

D vanishes by the implicit function theorem, $z''(\beta)|_{\beta=1} = 0$ when $\alpha \leq 1$. The physical interpretation is that a typical orbit will stick for long times near the $\overline{0}$ marginal fixed point, and the 'trapping time' will be larger for higher values of the intermittency parameter s (recall $\alpha = 1/s$). As always, we need to look more closely at the behavior of traces of high powers of the transfer operator.

The evaluation of transport coefficient requires one more derivative with respect to expectation values of state space observables (see sect. 25.1): if we use the diffusion dynamical zeta function (25.7), we may write the diffusion coefficient as an inverse Laplace transform, in such a way that the distinction between maps and flows has vanished. In the case of $1 - dimensional$ diffusion we thus have

$$D = \lim_{t\to\infty} \frac{d^2}{d\beta^2} \frac{1}{2\pi i} \int_{a-i\infty}^{a+i\infty} ds \, e^{st} \frac{\zeta'(\beta, s)}{\zeta(\beta, s)}\bigg|_{\beta=0} \tag{25.32}$$

where the ζ' refers to the derivative with respect to s.

The evaluation of inverse Laplace transforms for high values of the argument is most conveniently performed using Tauberian theorems. We shall take

$$\omega(\lambda) = \int_0^\infty dx\, e^{-\lambda x} u(x),$$

with $u(x)$ monotone as $x \to \infty$; then, as $\lambda \mapsto 0$ and $x \mapsto \infty$ respectively (and $\rho \in (0, \infty)$),

$$\omega(\lambda) \sim \frac{1}{\lambda^\rho} L\left(\frac{1}{\lambda}\right)$$

if and only if

$$u(x) \sim \frac{1}{\Gamma(\rho)} x^{\rho-1} L(x),$$

where L denotes any slowly varying function with $\lim_{t\to\infty} L(ty)/L(t) = 1$. Now

$$\frac{1/\zeta_0'(e^{-s}, \beta)}{1/\zeta_0(e^{-s}, \beta)} = \frac{\left(\frac{4}{\Lambda} + \frac{\Lambda-4}{\Lambda\zeta(1+\alpha)}\left(J(e^{-s}, \alpha+1) + J(e^{-s}, \alpha)\right)\right)\cosh\beta}{1 - \frac{4}{\Lambda}e^{-s}\cosh\beta - \frac{\Lambda-4}{\Lambda\zeta(1+\alpha)}e^{-s}(e^{-s}, \alpha+1)\cosh\beta J}.$$

Taking the second derivative with respect to β we obtain

$$\frac{d^2}{d\beta^2}\left(1/\zeta_0'(e^{-s}, \beta)/\zeta^{-1}(e^{-s}, \beta)\right)_{\beta=0}$$

$$= \frac{\frac{4}{\Lambda} + \frac{\Lambda-4}{\Lambda\zeta(1+\alpha)}\left(J(e^{-s}, \alpha+1) + J(e^{-s}, \alpha)\right)}{\left(1 - \frac{4}{\Lambda}e^{-s} - \frac{\Lambda-4}{\Lambda\zeta(1+\alpha)}e^{-s}J(e^{-s}, \alpha+1)\right)^2} = g_\alpha(s). \tag{25.33}$$

The asymptotic behavior of the inverse Laplace transform (25.32) may then be evaluated via Tauberian theorems, once we use our estimate for the behavior of Jonquière functions near $z = 1$. The deviations from normal behavior correspond to an explicit dependence of D on time. Omitting prefactors (which can be calculated by the same procedure) we have

$$g_\alpha(s) \sim \begin{cases} s^{-2} & \text{for } \alpha > 1 \\ s^{-(\alpha+1)} & \text{for } \alpha \in (0, 1) \\ 1/(s^2 \ln s) & \text{for } \alpha = 1. \end{cases}$$

The anomalous diffusion exponents follow:

<div style="text-align: right">exercise 25.6</div>

$$\langle(x - x_0)^2\rangle_t \sim \begin{cases} t^\alpha & \text{for } \alpha \in (0, 1) \\ t/\ln t & \text{for } \alpha = 1 \\ t & \text{for } \alpha > 1. \end{cases} \tag{25.34}$$

Résumé

With initial data accuracy $\delta x = |\delta \mathbf{x}(0)|$ and system size L, a trajectory is predictable only to the finite Lyapunov time $T_{\text{Lyap}} \approx \lambda^{-1} \ln |L/\delta x|$. Beyond that, chaos rules. We have discussed the implications in sect. 1.8: chaos is good news for prediction of long term observables such as transport in statistical mechanics.

The classical Boltzmann equation for evolution of 1-particle density is based on *stosszahlansatz*, neglect of particle correlations prior to, or after a 2-particle collision. It is a very good approximate description of dilute gas dynamics, but a difficult starting point for inclusion of systematic corrections. In the theory developed here, no correlations are neglected - they are all included in the cycle averaging formula such as the cycle expansion for the diffusion constant

$$
D = \frac{1}{2d} \frac{1}{\langle T \rangle_\zeta} \sum {}' (-1)^{k+1} \frac{(\hat{n}_{p_1} + \cdots + \hat{n}_{p_k})^2}{|\Lambda_{p_1} \cdots \Lambda_{p_k}|} \, .
$$

Such formulas are *exact*; the issue in their applications is what are the most effective schemes of estimating the infinite cycle sums required for their evaluation. Unlike most statistical mechanics, here there are no phenomenological macroscopic parameters; quantities such as transport coefficients are calculable to any desired accuracy from the microscopic dynamics.

For systems of a few degrees of freedom these results are on rigorous footing, but there are indications that they capture the essential dynamics of systems of many degrees of freedom as well.

Though superficially indistinguishable from the probabilistic random walk diffusion, deterministic diffusion is quite recognizable, at least in low dimensional settings, through fractal dependence of the diffusion constant on the system parameters, and through non-Gaussion relaxation to equilibrium (non-vanishing Burnett coefficients).

That Smale's "structural stability" conjecture turned out to be wrong is not a bane of chaotic dynamics - it is actually a virtue, perhaps the most dramatic experimentally measurable prediction of chaotic dynamics. As long as microscopic periodicity is exact, the prediction is counterintuitive for a physicist - transport coefficients are *not* smooth functions of system parameters, rather they are non-monotonic, *nowhere differentiable* functions.

Actual evaluation of transport coefficients is a test of the techniques developed above in physical settings. In cases of severe pruning the trace formulas and ergodic sampling of dominant cycles might be more effective strategy than the cycle expansions of dynamical zeta functions and systematic enumeration of all cycles.

Commentary

Remark 25.1 <u>Lorentz gas.</u>   The original pinball model proposed by Lorentz [25.4] consisted of randomly, rather than regularly placed scatterers.

Remark 25.2 <u>Who's dunnit?</u>   Cycle expansions for the diffusion constant of a particle moving in a periodic array have been introduced by R. Artuso [25.5] (exact dynamical zeta function for $1 - dimensional$ chains of maps (25.8)), by W.N. Vance [25.6],and by P. Cvitanović, J.-P. Eckmann, and P. Gaspard [25.7] (the dynamical zeta function cycle expansion (25.8) applied to the Lorentz gas).

Remark 25.3 <u>Lack of structural stability for D.</u>   Expressions like (25.20) may lead to an expectation that the diffusion coefficient (and thus transport properties) are smooth functions of the chaoticity of the system (parameterized, for example, by the Lyapunov exponent $\lambda = \ln \Lambda$). This turns out not to be true: D as a function of Λ is a fractal, nowhere differentiable curve shown in figure 25.5. The dependence of D on the map parameter Λ is rather unexpected - even though for larger Λ more points are mapped outside the unit cell in one iteration, the diffusion constant does not necessarily grow. We refer the reader to refs. [25.15, 25.16] for early work on the deterministic diffusion induced by 1-dimensional maps. The sawtooth map (25.9) was introduced by Grossmann and Fujisaka [25.17] who derived the integer slope formulas (25.20) for the diffusion constant. The sawtooth map is also discussed in refs. [25.18]. The fractal dependence of diffusion constant on the map parameter is discussed in refs. [25.9, 25.8, 25.10]. Sect. 1.8 gives a brief summary of the experimental implications; for the the current state of the art of fractal transport coefficients consult the first part of Klage's monograph [25.12]. Would be nice if someone would eventually check these predictions in experiments... Statistical mechanicians tend to believe that such complicated behavior is not to be expected in systems with very many degrees of freedom, as the addition to a large integer dimension of a number smaller than 1 should be as unnoticeable as a microscopic perturbation of a macroscopic quantity. No fractal-like behavior of the conductivity for the Lorentz gas has been detected so far [25.14].   (P. Cvitanović and L. Rondoni)

Remark 25.4 <u>Symmetry factorization in one dimension.</u>   In the $\beta = 0$ limit the dynamics (25.11) is symmetric under $x \to -x$, and the zeta functions factorize into products of zeta functions for the symmetric and antisymmetric subspaces, as described in sect. 21.1.1:

$$
\begin{aligned}
\frac{1}{\zeta(0,z)} &= \frac{1}{\zeta_s(0,z)} \frac{1}{\zeta_a(0,z)} \\
\frac{\partial}{\partial z} \frac{1}{\zeta} &= \frac{1}{\zeta_s} \frac{\partial}{\partial z} \frac{1}{\zeta_a} + \frac{1}{\zeta_a} \frac{\partial}{\partial z} \frac{1}{\zeta_s} .
\end{aligned}
\tag{25.35}
$$

The leading (material flow conserving) eigenvalue $z = 1$ belongs to the symmetric subspace $1/\zeta_s(0,1) = 0$, so the derivatives (25.15) also depend only on the symmetric subspace:

$$
\begin{aligned}
\langle n \rangle_\zeta &= \left. z \frac{\partial}{\partial z} \frac{1}{\zeta(0,z)} \right|_{z=1} \\
&= \left. \frac{1}{\zeta_a(0,z)} z \frac{\partial}{\partial z} \frac{1}{\zeta_s(0,z)} \right|_{z=1} .
\end{aligned}
\tag{25.36}
$$

length	# cycles	$\zeta(0,0)$	λ
1	5	-1.216975	-
2	10	-0.024823	1.745407
3	32	-0.021694	1.719617
4	104	0.000329	1.743494
5	351	0.002527	1.760581
6	1243	0.000034	1.756546

Table 25.1: Fundamental domain, w=0.3 .

Implementing the symmetry factorization is convenient, but not essential, at this level of computation.

Remark 25.5 <u>Lorentz gas in the fundamental domain.</u>   The vector valued nature of the generating function (25.3) in the case under consideration makes it difficult to perform a calculation of the diffusion constant within the fundamental domain. Yet we point out that, at least as regards scalar quantities, the full reduction to $\tilde{\mathcal{M}}$ leads to better estimates. A proper symbolic dynamics in the fundamental domain has been introduced in ref. [25.19].

In order to perform the full reduction for diffusion one should express the dynamical zeta function (25.7) in terms of the prime cycles of the fundamental domain $\tilde{\mathcal{M}}$ of the lattice (see figure 25.2) rather than those of the elementary (Wigner-Seitz) cell $\mathcal{M}$. This problem is complicated by the breaking of the rotational symmetry by the auxiliary vector β, or, in other words, the non-commutativity of translations and rotations: see ref. [25.7].

Remark 25.6   <u>Anomalous diffusion.</u>   Anomalous diffusion for $1-dimensional$ intermittent maps was studied in the continuous time random walk approach in refs. [24.10, 24.11]. The first approach within the framework of cycle expansions (based on truncated dynamical zeta functions) was proposed in ref. [24.12]. Our treatment follows methods introduced in ref. [24.13], applied there to investigate the behavior of the Lorentz gas with unbounded horizon.

Remark 25.7   <u>Jonquière functions.</u>   In statistical mechanics Jonquière function (25.29) appears in the theory of free Bose-Einstein gas, see refs. [24.22, 24.23].

Exercises

25.1. **Diffusion for odd integer Λ.** Show that when the slope $\Lambda = 2k-1$ in (25.9) is an odd integer, the diffusion constant is given by $D = (\Lambda^2 - 1)/24$, as stated in (25.21).

25.2. **Fourth-order transport coefficient.** Verify (25.24). You will need the identity

$$\sum_{k=1}^{n} k^4 = \frac{1}{30}n(n+1)(2n+1)(3n^2 + 3n - 1).$$

25.3. **Finite Markov partitions.** Verify (25.28).

25.4. **Maps with variable peak shape:** Consider the following piecewise linear map

$$f_\delta(x) = \begin{cases} \frac{3x}{1-\delta} & x \in \mathcal{M}_1 \\ \frac{3}{2} - \left(\frac{2}{\delta}\left|\frac{4-\delta}{12} - x\right|\right) & x \in \mathcal{M}_2 \quad (25.37) \\ 1 - \frac{3}{1-\delta}\left(x - \frac{1}{6}(2+\delta)\right) & x \in \mathcal{M}_3 \end{cases}$$

where $\mathcal{M}_1 = \left[0, \frac{1}{3}(1-\delta)\right]$, $\mathcal{M}_2 = \left[\frac{1}{3}(1-\delta), \frac{1}{6}(2+\delta)\right]$, $\mathcal{M}_3 = \left[\frac{1}{6}(2+\delta), \frac{1}{2}\right]$, and the map in $[1/2, 1]$ is obtained by antisymmetry with respect to $x = 1/2$, $y = 1/2$, Write the corresponding dynamical zeta function relevant to diffusion and then show that

$$D = \frac{\delta(2+\delta)}{4(1-\delta)}$$

See refs. [25.21, 25.22] for further details.

25.5. **Two-symbol cycles for the Lorentz gas.** Write down all cycles labeled by two symbols, such as (0 6), (1 7), (1 5) and (0 5).

ChaosBook.org/pages offers several project-length deterministic diffusion exercises.

25.6. **Accelerated diffusion.** (medium difficulty) Consider a map h, such that $\hat{h} = \hat{f}$ of figure 25.6 (b), but now running branches are turned into standing branches and vice versa, so that $1, 2, 3, 4$ are standing while 0 leads to both positive and negative jumps. Build the corresponding dynamical zeta function and show that

$$\sigma^2(t) \sim \begin{cases} t & \text{for } \alpha > 2 \\ t \ln t & \text{for } \alpha = 2 \\ t^{3-\alpha} & \text{for } \alpha \in (1, 2) \\ t^2/\ln t & \text{for } \alpha = 1 \\ t^2 & \text{for } \alpha \in (0, 1) \end{cases}$$

25.7. **Recurrence times for Lorentz gas with infinite horizon.** Consider the Lorentz gas with unbounded horizon with a square lattice geometry, with disk radius R and unit lattice spacing. Label disks according to the (integer) coordinates of their center: the sequence of recurrence times $\{t_j\}$ is given by the set of collision times. Consider orbits that leave the disk sitting at the origin and hit a disk far away after a free flight (along the horizontal corridor). Initial conditions are characterized by coordinates (ϕ, α) (ϕ determines the initial position along the disk, while α gives the angle of the initial velocity with respect to the outward normal: the appropriate measure is then $d\phi \cos \alpha \, d\alpha$ ($\phi \in [0, 2\pi)$, $\alpha \in [-\pi/2, \pi/2]$. Find how $\phi(T)$ scales for large values of T: this is equivalent to investigating the scaling of portions of the state space that lead to a first collision with disk $(n, 1)$, for large values of n (as $n \mapsto \infty$ $n \simeq T$).

25.8. **Diffusion reduced to the fundamental domain.** Maps such as figure 25.3 are antisymmetric. Reduce such antisymmetric maps as in example 9.3, and write down the formula (25.14) for the diffusion constant D in terms of the fundamental domain cycles (relative periodic orbits) alone (P. Gaspard says it cannot be done [25.7]).

References

[25.1] J. Machta and R. Zwanzig, *Phys. Rev. Lett.* **50**, 1959 (1983).

[25.2] G.P. Morriss and L. Rondoni, *J. Stat. Phys.* **75**, 553 (1994).